


 Cite this: *Nanoscale*, 2020, **12**, 16091

## Two unusual nanosized Nd<sup>3+</sup>-substituted selenotungstate aggregates simultaneously comprising lacunary Keggin and Dawson polyoxotungstate segments†

 Hailou Li,<sup>a,b</sup> Chen Lian,<sup>b</sup> Lijuan Chen,<sup>\*a</sup> Junwei Zhao <sup>\*a</sup> and Guo-Yu Yang <sup>\*b</sup>

Two unique nanosized Nd<sup>3+</sup>-substituted selenotungstates Na<sub>9</sub>K<sub>8</sub>{[W<sub>3</sub>Nd<sub>2</sub>(H<sub>2</sub>O)<sub>3</sub>(NO<sub>3</sub>)O<sub>6</sub>](B-α-SeW<sub>9</sub>O<sub>33</sub>)<sub>2</sub>(α-Se<sub>2</sub>W<sub>14</sub>O<sub>52</sub>)}·35H<sub>2</sub>O (**1**) and [H<sub>2</sub>N(CH<sub>3</sub>)<sub>2</sub>]<sub>7</sub>H<sub>9</sub>Na<sub>4</sub>{[W<sub>2</sub>Nd<sub>2</sub>(H<sub>2</sub>O)<sub>8</sub>O<sub>6</sub>(OH)<sub>2</sub>(β-Se<sub>2</sub>W<sub>14</sub>O<sub>52</sub>)] [W<sub>3</sub>Nd<sub>2</sub>(H<sub>2</sub>O)<sub>6</sub>O<sub>7</sub>(B-α-SeW<sub>9</sub>O<sub>33</sub>)<sub>2</sub>]}·84H<sub>2</sub>O (**2**) were prepared by reacting NaSeO<sub>3</sub>, Na<sub>2</sub>WO<sub>4</sub>·2H<sub>2</sub>O with Nd(NO<sub>3</sub>)<sub>3</sub>·6H<sub>2</sub>O in aqueous solution by controlling different cations and pH values. **1** was synthesized at pH = 4.3 in the presence of KCl, whereas **2** was synthesized at pH = 3.0 in the presence of [H<sub>2</sub>N(CH<sub>3</sub>)<sub>2</sub>]<sub>7</sub>Cl. The most striking structural feature of **1** and **2** is the coexistence of vacant Keggin and Dawson segments in the polyoxoanion, which is extremely rare in the field of polyoxometalate chemistry. The trimeric polyoxoanion of **1** can be perceived as a fusion of one α-type tetravacant Dawson [α-Se<sub>2</sub>W<sub>14</sub>O<sub>52</sub>]<sup>14-</sup> unit and two trivacant Keggin [B-α-SeW<sub>9</sub>O<sub>33</sub>]<sup>8-</sup> segments sealing a trigonal bipyramid pentanuclear [W<sub>3</sub>Nd<sub>2</sub>(H<sub>2</sub>O)<sub>3</sub>(NO<sub>3</sub>)O<sub>6</sub>]<sup>11+</sup> cluster, while the pentameric polyoxoanion of **2** can be described as one β-type tetravacant Dawson [β-Se<sub>2</sub>W<sub>14</sub>O<sub>52</sub>]<sup>14-</sup> fragment and four trivacant Keggin [B-α-SeW<sub>9</sub>O<sub>33</sub>]<sup>8-</sup> segments anchoring a saddle-shaped [W<sub>8</sub>Nd<sub>6</sub>(H<sub>2</sub>O)<sub>20</sub>O<sub>20</sub>(OH)<sub>2</sub>]<sup>24+</sup> cluster. In addition, the measurements of catalytic oxidation of aromatic thioethers show that **2** as a catalyst possesses extremely outstanding catalytic performance under mild reaction conditions.

 Received 27th May 2020,  
 Accepted 6th July 2020

DOI: 10.1039/d0nr04051g

[rsc.li/nanoscale](http://rsc.li/nanoscale)

## Introduction

The continuous development of and search for high-efficiency selective catalytic oxidation of aromatic sulfides has drawn tremendous attention due to their corresponding sulfoxidation products (sulfoxides and sulfones) that have widely been utilized as pivotal synthetic intermediates in organic catalysis, medicine and oxygen-transfer reactions.<sup>1–7</sup> In the sulfide oxidation reactions involving polyoxometalates (POMs) as catalysts, hydrogen peroxide (H<sub>2</sub>O<sub>2</sub>) generally serves as a “green” oxidant with the merits of low cost, eco-friendliness and high efficiency, indicating that Lewis acidity of POMs together with the oxidation of hydrogen peroxide can synergistically improve the catalytic reaction systems.<sup>8–10</sup>

POMs, as an important class of polynuclear metal–oxo clusters, exhibit tremendous structural diversities, remarkable physicochemical properties and colossal potential applications in catalysis, biology, optics, magnetism and electrochemistry.<sup>11–14</sup> From the viewpoint of structural chemistry, continuous developments and fruitful achievements of new POM-based materials largely depend upon available and diverse lacunary POM building units because they can provide abundant bonding sites for capturing additional metal ions to derive innovative higher-nuclear mixed-metal clusters and bring about unpredictable functionalities. Within this field, lacunary Keggin and Dawson POM building units play a significant role in enriching the structural chemistry of POMs and are ubiquitously used as purely inorganic and multidentate O-donor ligands in the construction of novel POM-based functional materials.<sup>15,16</sup> In fact, the key to the assembly and functionalization of POM-based materials rests on the heteroatom species that can template the construction of structures; moreover, heteroatoms’ electronic configurations can also have a major impact on the structural assembly of desired outcomes and sometimes endow the POM skeletons in the process with specific functionalities.<sup>17</sup> Recently, the lone-pair-containing Se<sup>IV</sup> heteroatom has been widely employed in the preparation of gigantic poly(POM)s since the combination of

<sup>a</sup>Henan Key Laboratory of Polyoxometalate Chemistry, College of Chemistry and Chemical Engineering, Henan University, Kaifeng, Henan 475004, China.

E-mail: ljchen@henu.edu.cn, zhaojunwei@henu.edu.cn

<sup>b</sup>MOE Key Laboratory of Cluster Science, School of Chemistry and Chemical Engineering, Beijing Institute of Technology, Beijing 102488, China.

E-mail: ygy@bit.edu.cn

† Electronic supplementary information (ESI) available: The refinement details and additional figures. CCDC 1942924 and 1942927. For ESI and crystallographic data in CIF or other electronic format see DOI: 10.1039/d0nr04051g

the lone-electron pair stereochemical effect  $\{\text{SeO}_3\}$  group with POM fragments can form open-framework selenotungstate (ST) intermediates, which is conducive to direct the incorporation of additional metal ions into the defective ST skeletons, allowing the assembly of, particularly, the-second-metal functionalized nanosized poly(ST) architectures.<sup>18,19</sup> To date, some prominent nanosized poly(ST) species have been discovered,<sup>17–29</sup> the majority of which usually contain one type of heteropolyoxotungstate (HPOT) building unit (either Keggin-type or Dawson-type) in their structures; however, related reports on nanosized poly(ST) species concurrently consisting of two types of HPOT building units are extremely unwarranted.<sup>30,31</sup> Therefore, the exploration and preparation of nanosized poly(POM) aggregates including two or more kinds of architecturally distinct HPOT units have triggered an ever-increasing concern, which can offer a great possibility for constructing innovative poly(POM) species with unexpected properties. Inspired by these ideas, as for the ST system, discovering and preparing novel rare-earth (RE)-substituted poly(ST) species assembled from lacunary Keggin and Dawson units are still of great significance and challenging. Recently, the convenient one-pot self-assembly strategy of simple materials in dexterously assembling giant POM-based cluster materials has shown noticeable advantages. In such flexible reaction circumstances, the elaborate selection of heteroatoms with the lone-electron pair stereochemical effect is of fundamental importance. To enhance the possibility of generating two or more types of HPOT building units, the structure-directing effect of the trigonal pyramidal  $\{\text{SeO}_3\}$  template is very crucial as it can structurally direct the aggregation of  $\{\text{WO}_6\}$  groups into various vacant POM nucleophiles. It is well known that the formation of different POM fragments is closely related to the pH of the reaction system, and as a result, the pH range of 3–5 should be controlled, the major reason for which is that lacunary Keggin or Dawson ST fragments may coexist under these conditions according to the previous results of the W–Se–O system.<sup>17,18,22,27,30</sup> Additionally, big ionic radius RE cations with a variable coordination number and poor stereochemical preference can prevent them from being fully encapsulated into the lacunary sites of ST building units, thereby facilitating the aggregation of different lacunary ST nucleophiles through the residual coordination sites of RE cations and other bridging units. According to the principle of radius matching of anions and cations, to stabilize the structures of nanosized RE-substituted poly(ST) aggregates containing mixed HPOT units, some counter-cation components with a large ion radius should be introduced to the reaction system. Thus, KCl and  $[\text{H}_2\text{N}(\text{CH}_3)_2]\text{-Cl}$  were utilized in the synthetic process. By elaborately controlling the reaction parameters (such as reactants, pH, counter-cations, *etc.*), herein, two novel  $\text{Nd}^{3+}$  substituted poly(ST) aggregates containing mixed Keggin and Dawson segments  $\text{Na}_9\text{K}_8\{[\text{W}_3\text{Nd}_2(\text{H}_2\text{O})_3(\text{NO}_3)_6][\text{B-}\alpha\text{-SeW}_9\text{O}_{33})_2(\alpha\text{-Se}_2\text{W}_{14}\text{O}_{52})]\cdot 35\text{H}_2\text{O}$  (**1**) and  $[\text{H}_2\text{N}(\text{CH}_3)_2]_7\text{H}_9\text{Na}_4\{[\text{W}_2\text{Nd}_2(\text{H}_2\text{O})_8\text{O}_6(\text{OH})_2(\beta\text{-Se}_2\text{W}_{14}\text{O}_{52})][\text{W}_3\text{Nd}_2(\text{H}_2\text{O})_6\text{O}_7(\text{B-}\alpha\text{-SeW}_9\text{O}_{33})_2]\}_2\cdot 84\text{H}_2\text{O}$  (**2**) have been obtained in aqueous solution by means of controlling different counter-cations and pH and characterized by single-

crystal X-ray diffraction, PXRD, TGA and IR spectra. **1** was synthesized at pH = 4.3 in the presence of KCl, whereas **2** was synthesized at pH = 3.0 in the presence of  $[\text{H}_2\text{N}(\text{CH}_3)_2]\text{-Cl}$ . As expected, both are constructed from mixed vacant Keggin and Dawson units incorporated with  $\text{Nd}^{3+}$  cations. Furthermore, **2** as a catalyst exhibits prominent catalytic activity and recyclability for the oxidation of thioether species under mild reaction conditions.

## Experimental

### Preparation of $\text{Na}_9\text{K}_8\{[\text{W}_3\text{Nd}_2(\text{H}_2\text{O})_3(\text{NO}_3)_6][\text{B-}\alpha\text{-SeW}_9\text{O}_{33})_2(\alpha\text{-Se}_2\text{W}_{14}\text{O}_{52})]\cdot 35\text{H}_2\text{O}$ (**1**)

$\text{Na}_2\text{WO}_4\cdot 2\text{H}_2\text{O}$  (1.203 g, 3.647 mmol),  $\text{Na}_2\text{SeO}_3$  (0.051 g, 0.295 mmol) and KCl (0.306 g, 4.107 mmol) were dissolved in 20 mL of distilled water. The solution was stirred for 10 min and its pH was set to 4.3 by adding the HCl solution (6.0 mol  $\text{L}^{-1}$ ) dropwise. Subsequently,  $\text{Nd}(\text{NO}_3)_3\cdot 6\text{H}_2\text{O}$  (0.054 g, 0.123 mmol) was added and the pH was readjusted to 4.30. After stirring for 30 min, the final solution (pH = 4.6) was filtered and left at ambient temperature. Slow evaporation resulted in purple prism crystals of **1** for one month. Yield: 0.180 g (28.44%) based on  $\text{Nd}(\text{NO}_3)_3\cdot 6\text{H}_2\text{O}$ . Anal. calcd (%): H 0.74, N 0.14, Na 2.01, K 3.04, Se 3.07, Nd 2.80, W 62.54; found: H 0.90, N 0.08, Na 2.18, K 2.91, Se 3.16, Nd 2.73, W 62.78.

### Preparation of $[\text{H}_2\text{N}(\text{CH}_3)_2]_7\text{H}_9\text{Na}_4\{[\text{W}_2\text{Nd}_2(\text{H}_2\text{O})_8\text{O}_6(\text{OH})_2(\beta\text{-Se}_2\text{W}_{14}\text{O}_{52})][\text{W}_3\text{Nd}_2(\text{H}_2\text{O})_6\text{O}_7(\text{B-}\alpha\text{-SeW}_9\text{O}_{33})_2]\}_2\cdot 84\text{H}_2\text{O}$ (**2**)

$\text{Na}_2\text{WO}_4\cdot 2\text{H}_2\text{O}$  (4.003 g, 12.136 mmol),  $\text{Na}_2\text{SeO}_3$  (0.204 g, 1.180 mmol) and  $[\text{H}_2\text{N}(\text{CH}_3)_2]\text{-Cl}$  (1.996 g, 24.480 mmol) were dissolved in 30 mL of distilled water. The solution was stirred for 10 min and its pH was set to 3.0 by adding the HCl solution (6.0 mol  $\text{L}^{-1}$ ) dropwise. And then  $\text{Nd}(\text{NO}_3)_3\cdot 6\text{H}_2\text{O}$  (0.5003 g, 1.141 mmol) was introduced into the solution and the pH was readjusted to 3.0. After stirring for 30 min, the final solution (pH = 3.2) was filtered and left at ambient temperature. Slow evaporation of the filtrate resulted in purple block crystals of **2** for three weeks. Yield: 0.785 g (23.48%) based on  $\text{Nd}(\text{NO}_3)_3\cdot 6\text{H}_2\text{O}$ . Anal. calcd (%): H 1.58, C 0.96 N 0.56, Na 0.52, Se 2.69, Nd 4.92, W 60.59; found: H 1.75, C 1.09 N 0.41, Na 0.68, Se 2.52, Nd 4.85, W 60.37.

## Results and discussion

### Synthesis discussion

The nanosized poly(POM) aggregates formed by copolymerization of two or more kinds of structurally distinct HPOT units have attracted increasing attention. Upon our continuous work with aiming at discovering novel RE<sup>3+</sup> substituted STs consisting of lacunary Keggin and Dawson units, **1** and **2** were successfully synthesized based on the reactions of  $\text{Na}_2\text{WO}_4\cdot 2\text{H}_2\text{O}$ ,  $\text{Na}_2\text{SeO}_3$  and  $\text{Nd}(\text{NO}_3)_3\cdot 6\text{H}_2\text{O}$  under weak acid conditions by controlling different cations and pH values. In the preparation

process, the pH value is a significant factor affecting the reaction and structural construction of products. Paralleling investigations indicate that the pH range of 4.1–4.6 and 2.8–3.2 are helpful for the formation of **1** and **2**, respectively. The optimal pH value for **1** and **2** are 4.3 and 3.0. Furthermore, the counter-cations also play a very important role in the synthetic process. KCl was used for the preparation of **1**, whereas  $[\text{H}_2\text{N}(\text{CH}_3)_2]\text{-Cl}$  was utilized for the preparation of **2**. In addition, in order to obtain similar structures by replacing the  $\{\text{SeO}_3\}$  group with other lone-electron pair stereochemical effect groups such as  $\{\text{AsO}_3\}$  and  $\{\text{SbO}_3\}$ , related experiments have been also performed under similar conditions and no similar structures were found. For example,  $\text{NaAsO}_2$  was a starting material under similar conditions, and an octameric multi- $\text{Nd}^{3+}$  substituted arsenotungstate  $\text{Na}_4[\text{H}_2\text{N}(\text{CH}_3)_2]_{18}\text{H}_{21}[\text{Nd}(\text{H}_2\text{O})_7][\text{W}_{16}\text{Nd}_{10}\text{O}_{50}(\text{H}_2\text{O})_{34}(\text{B-}\alpha\text{-AsW}_9\text{O}_{33})_8]\cdot 60\text{H}_2\text{O}$  only including trivacant Keggin HPOT segments was isolated.<sup>28</sup> When  $\text{SbCl}_3$  was employed to replace  $\text{Na}_2\text{SeO}_3$ , we could not obtain RE-substituted antimono-tungstate species.

### Structural description

The phase purity of **1** and **2** can be identified by the good consistency between their powder X-ray diffraction (PXRD) patterns and simulated patterns from single-crystal X-ray diffraction data (Fig. S1†).

Single-crystal X-ray diffraction indicates that both **1** and **2** crystallize in the triclinic space group  $P\bar{1}$  (Table 1) and show the coexistence of lacunary Keggin and Dawson segments in their polyoxoanions (POAs). The molecular structure of **1** consists of a mixed Keggin- and Dawson-type trimeric POA

$\{[\text{W}_3\text{Nd}_2(\text{H}_2\text{O})_3(\text{NO}_3)\text{O}_6](\text{B-}\alpha\text{-SeW}_9\text{O}_{33})_2(\alpha\text{-Se}_2\text{W}_{14}\text{O}_{52})\}^{17-}$  (**1a**), 9  $\text{Na}^+$  cations, 8  $\text{K}^+$  cations and 35 lattice water molecules. Bond valence sum (BVS) values<sup>32</sup> of O1 W, O2 W and O3 W located on the two  $\text{Nd}^{3+}$  cations are 0.262, 0.284 and 0.270, respectively, (Table S1†) so they are water ligands. **1a** (Fig. 1a) can be described as one tetravacant Dawson  $[\alpha\text{-Se}_2\text{W}_{14}\text{O}_{52}]^{12-}$  segment and two trivacant Keggin  $[\text{B-}\alpha\text{-SeW}_9\text{O}_{33}]^{8-}$  segments encapsulating a central trigonal bipyramid pentanuclear  $[\text{W}_3\text{Nd}_2(\text{H}_2\text{O})_3(\text{NO}_3)\text{O}_6]^{11+}$   $\{\text{Nd}_2\text{W}_3\}$  cluster (Fig. 1b) by means of 20  $\mu_2\text{-O}$  atoms. The tetravacant Dawson  $[\alpha\text{-Se}_2\text{W}_{14}\text{O}_{52}]^{12-}$  unit can be regarded as removing a ring-shaped apex-linked  $[\text{W}_4\text{O}_{10}(\text{H}_2\text{O})_2]^{4+}$  group from the equatorial position of the parent “saturated”  $[\alpha\text{-Se}_2\text{W}_{18}\text{O}_{62}(\text{H}_2\text{O})_2]^{8-}$  unit (Fig. 1c and f), and similar tetravacant Dawson segments have been observed by us.<sup>22,27</sup> The trivacant  $[\text{B-}\alpha\text{-SeW}_9\text{O}_{33}]^{8-}$  segment is composed of a central trigonal pyramidal  $\{\text{SeO}_3\}$  fragment and three edge-sharing  $\{\text{W}_3\text{O}_{13}\}$  groups (Fig. 1e).

Although the  $\{\text{Nd}_2\text{W}_3\}$  cluster of **1** (Fig. 1d and g) is resembled with that of previously reported  $[(\text{W}_3\text{Eu}_2(\text{H}_2\text{O})_8\text{AsO}_8(\text{OH}))(\text{B-}\alpha\text{-AsW}_9\text{O}_{33})_2]_2^{16-}$  (**3**),<sup>33</sup> in which three W atoms stand on the basal plane and two  $\text{Eu}^{3+}$  cations are situated at two vertexes. While the conspicuous discrepancies lie in the following three points: (a) the coordination numbers of RE cations are different,  $\text{Nd}^{3+}$  and  $\text{Nd}^{2+}$  cations in the  $\{\text{Nd}_2\text{W}_3\}$  cluster of **1** are deca-coordinate and nona-coordinate, respectively, whereas both  $\text{Eu}^{3+}$  cations in the  $\{\text{Eu}_2\text{W}_3\}$  cluster of **3** are octa-coordinate; (b) the  $\{\text{Nd}_2\text{W}_3\}$  cluster of **1** contains an inorganic  $\text{NO}_3^-$  chelating ligand, while **3** does not; (c) the  $\{\text{Nd}_2\text{W}_3\}$  cluster of **1** connects one  $[\alpha\text{-Se}_2\text{W}_{14}\text{O}_{52}]^{12-}$  unit and two  $[\text{B-}\alpha\text{-SeW}_9\text{O}_{33}]^{8-}$  segments by 20  $\mu_2\text{-O}$  atoms, while the

**Table 1** Crystallographic data and structural refinements for **1** and **2**

	<b>1</b>	<b>2</b>
Empirical formula	$\text{H}_{76}\text{K}_8\text{NNa}_9\text{Nd}_2\text{O}_{165}\text{Se}_4\text{W}_{35}$	$\text{C}_{14}\text{H}_{275}\text{N}_7\text{Na}_4\text{Nd}_6\text{O}_{310}\text{Se}_6\text{W}_{58}$
Fw	10 289.40	17 597.87
Crystal system	Triclinic	Triclinic
Space group	$P\bar{1}$	$P\bar{1}$
$a$ , Å	18.6658(16)	19.6262(15)
$b$ , Å	21.9717(19)	28.530(2)
$c$ , Å	22.0792(19)	30.005(2)
$\alpha$ , °	71.751(2)	90.355(2)
$\beta$ , °	67.1190(10)	99.225(2)
$\gamma$ , °	68.721(2)	94.2750(10)
$V$ , Å <sup>3</sup>	7616.1(11)	16 535(2)
$Z$	2	2
$\mu$ , mm <sup>-1</sup>	28.301	21.781
$F(000)$	9000	15 572
$T$ , K	296(2)	296(2)
Limiting indices	$-22h \leq 22$ $-26k \leq 16$ $-26l \leq 26$	$-23h \leq 23$ $-31k \leq 33$ $-35l \leq 32$
No. of reflections collected	37 242	84 730
No. of independent reflections	25 865	57 841
$R_{\text{int}}$	0.0616	0.1029
Data/restraints/parameters	25 865/366/1744	57 841/595/2643
Goodness-of-fit on $F^2$	1.062	1.028
Final $R$ indices [ $I > 2\sigma(I)$ ]	$R_1 = 0.0757$ $wR_2 = 0.1845$	$R_1 = 0.1193$ $wR_2 = 0.2551$
$R$ indices (all data)	$R_1 = 0.1135$ $wR_2 = 0.2006$	$R_1 = 0.2362$ $wR_2 = 0.2926$

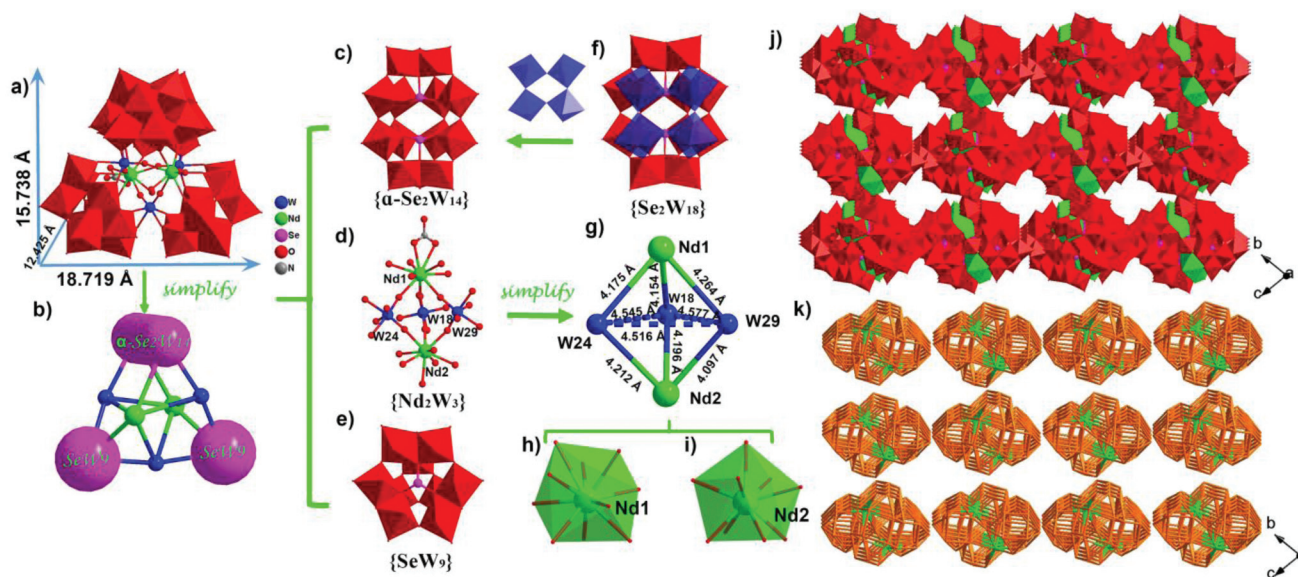


**Fig. 1** (a) View of the POA of **1**. (b) Simplified view of the POA of **1**. (c) The tetravacant Dawson-type  $[\alpha\text{-Se}_2\text{W}_{14}\text{O}_{52}]^{12-}$  fragment. (d) View of the pentanuclear  $\{\text{Nd}_2\text{W}_3\}$  cluster. (e) The trivacant  $[\text{B-}\alpha\text{-SeW}_9\text{O}_{33}]^{8-}$  segment. (f) The "saturated"  $[\text{Se}_2\text{W}_{18}\text{O}_{62}(\text{H}_2\text{O})_2]^{8-}$  unit. (g) Simplified view of the trigonal bipyramid  $\{\text{Nd}_2\text{W}_3\}$  cluster. (h) The deca-coordinate  $\text{Nd}^{13+}$  cation. (i) The nona-coordinate  $\text{Nd}^{23+}$  cation. (j) View of the stacking of **1a** POAs along the *a* axis. (k) Simplified view of the stacking of **1a** POAs along the *a* axis.

$\{\text{Eu}_2\text{W}_3\}$  cluster of 3 combines two  $[\text{B-}\alpha\text{-AsW}_9\text{O}_{33}]^{9-}$  segments through 12  $\mu_2\text{-O}$  atoms (Fig. S2†). In the  $\{\text{Nd}_2\text{W}_3\}$  cluster, the W18 atom is combined with two  $[\text{B-}\alpha\text{-SeW}_9\text{O}_{33}]^{8-}$  segments *via* four  $\mu_2\text{-O}$  atoms [W–O: 1.916(17)–2.157(19) Å] and two  $\text{Nd}^{3+}$  cations *via* two  $\mu_2\text{-O}$  atoms [W–O: 1.696(15)–1.72(2) Å]. The W24 and W29 atoms show similar linking patterns, therefore only the W24 atom is described as a representative. The W24 atom links to one  $[\text{B-}\alpha\text{-SeW}_9\text{O}_{33}]^{8-}$  segment through two  $\mu_2\text{-O}$  atoms [W–O: 1.96(2)–2.170(17) Å], two  $\text{Nd}^{3+}$  cations *via* two  $\mu_2\text{-O}$  atoms [W–O: 1.721(17)–1.760(18) Å] and one  $[\alpha\text{-Se}_2\text{W}_{14}\text{O}_{52}]^{12-}$  unit by two  $\mu_2\text{-O}$  atoms [W–O: 1.882(19)–2.225(18) Å]. The deca-coordinate  $\text{Nd}^{13+}$  cation is defined by two  $\mu_2\text{-O}$  atoms from one  $[\text{B-}\alpha\text{-SeW}_9\text{O}_{33}]^{8-}$  segment [Nd–O: 2.55(2)–2.62(2) Å], three  $\mu_2\text{-O}$  atoms from three  $\{\text{WO}_6\}$  octahedra (W18, W24 and W29) [Nd–O: 2.475(15)–2.62(2) Å], two  $\mu_2\text{-O}$  atoms from  $[\alpha\text{-Se}_2\text{W}_{14}\text{O}_{52}]^{12-}$  unit [Nd–O: 2.44(2)–2.445(19) Å], two  $\mu_2\text{-O}$  atoms from  $\text{NO}_3^-$  [Nd–O: 2.63(2)–2.81(3) Å] and one terminal water ligand [Nd–O: 2.590(19) Å]. The nona-coordinate  $\text{Nd}^{23+}$  cation is resembled with the  $\text{Nd}^{13+}$  cation and the difference rests on the fact that the  $\text{Nd}^{13+}$  cation links one terminal coordination water molecule and one  $\text{NO}_3^-$  anion, while the  $\text{Nd}^{23+}$  cation joins two aqua ligands without  $\text{NO}_3^-$ . To our knowledge, carbonate chelating POMs have been commonly seen;<sup>34–36</sup> however, nitrate-involving POMs are extremely rare. Besides, the side lengths of the trigonal bipyramid  $\{\text{Nd}_2\text{W}_3\}$  cluster are in the range of 4.097–4.577 Å [W–W: 4.516–4.577 Å, Nd–W: 4.097–4.264 Å].

Moreover, in **1a** POA, we can easily find the familiar dimeric  $\{\text{Nd}_2\text{W}_3(\text{B-}\alpha\text{-SeW}_9\text{O}_{33})_2\}$  moieties, in which three W and two  $\text{Nd}^{3+}$  centers are usually used as connection points to expand the bonding with other clusters to form novel

architectures.<sup>37,38</sup> Here, four atoms (W24, W29, Nd1 and Nd2) in this dimer are inserted in the vacant sites of tetravacant  $[\alpha\text{-Se}_2\text{W}_{14}\text{O}_{52}]^{12-}$  fragment to generate a rare Keggin and Dawson mixed trimer. As far as we know, these mixed Keggin and Dawson RE-substituted trimers are very rare in POM chemistry,<sup>30</sup> although there are some reports on RE-substituted trimers comprising one type of HPOT building unit in their structures.<sup>29,39,40</sup>

Furthermore, the POA of **1** can also be described as two  $\text{Nd}^{3+}$  cations incorporated with a cyclic trimer, which is composed of one tetravacant  $[\alpha\text{-Se}_2\text{W}_{14}\text{O}_{52}]^{12-}$  unit and two trivacant  $[\text{B-}\alpha\text{-SeW}_9\text{O}_{33}]^{8-}$  segments through three octahedral  $\{\text{WO}_6\}$  linkers (Fig. S3†). In addition, it can be seen from the 3D packing arrangement viewed along the *a* axis that **1a** POAs are closely aligned in the mode of –A–A– with a distance of 18.66 Å. Along the *b* and *c* axes, the strict arrangements of POAs are both in the fashion of –A–B–A– with the distances of 21.97 Å and 22.08 Å, respectively (Fig. 1j and k, S4†).

The molecular structure of **2** is built by a mixed Keggin and Dawson pentameric POA  $\{[\text{W}_2\text{Nd}_2(\text{H}_2\text{O})_8\text{O}_6(\text{OH})_2(\beta\text{-Se}_2\text{W}_{14}\text{O}_{52})][\text{W}_3\text{Nd}_2(\text{H}_2\text{O})_6\text{O}_7(\text{B-}\alpha\text{-SeW}_9\text{O}_{33})_2]_2\}^{20-}$  (**2a**), 7  $[\text{H}_2\text{N}(\text{CH}_3)_2]^+$  cations, 9 protons, 4  $\text{Na}^+$  cations and 84 lattice water molecules. The BVS calculations show that the terminal oxygens on the  $\text{Nd}^{3+}$  cations in **2** are coordination water molecules (Table S2†), and BVS values of O14 W on W58 and O20 W on W27 are 0.404 and 0.332, respectively, so they are also coordination water molecules. Furthermore, BVS values of two  $\mu_2\text{-O}$  atoms (O94 and O172) connecting W4 and W26, and W16 and W47 are 0.995 and 1.098, respectively, indicating that they are monoprotonated oxygen atoms. The **2a** POA is a hexanuclear  $\text{Nd}^{3+}$  incorporated with a pentameric architecture  $\{[\text{W}_2\text{Nd}_2(\text{H}_2\text{O})_8$

$O_6(OH)_2(\beta\text{-Se}_2W_{14}O_{52})[W_3Nd_2(H_2O)_6O_7(SeW_9O_{33})_2]^{20-}$  (Fig. 2a-c) that is fabricated by one tetravacant Dawson  $[\beta\text{-Se}_2W_{14}O_{52}]^{12-}$  fragment, four trivacant Keggin  $[B\text{-}\alpha\text{-SeW}_9O_{33}]^{8-}$  segments and a central saddle-shaped cluster  $[W_8Nd_6(H_2O)_{20}O_{20}(OH)_2]^{24+}$   $\{Nd_6W_8\}$ . The  $[B\text{-}\alpha\text{-SeW}_9O_{33}]^{8-}$  and  $[\beta\text{-Se}_2W_{14}O_{52}]^{12-}$  fragments are distributed in the outer side of the saddle-shaped  $\{Nd_6W_8\}$  cluster (Fig. 2d-f), and install on it by means of 34  $\mu_2\text{-O}$  atoms. The tetravacant  $[\beta\text{-Se}_2W_{14}O_{52}]^{12-}$  fragment in **2** is different from the tetravacant  $[\alpha\text{-Se}_2W_{14}O_{52}]^{12-}$  segment in **1**, which can be considered to be formed by rotating  $60^\circ$  of two  $\{W_3\}$  trimers on two polar positions of **1** (Fig. 2h). As far as we know, the  $\beta$ -type tetravacant Dawson-type fragment is rarely observed in the field of POM chemistry. The saddle-shaped cluster can be thought of as a quadrilateral  $\{Nd_2W_2\}$  fragment (Fig. 2g) linking two trigonal bipyramid pentanuclear  $\{Nd_2W_3\}$  clusters in the *cis* configuration, which is extremely uncommon in coordination chemistry. The quadrilateral  $\{Nd_2W_2\}$  metal centers occupy four active sites at the equator of the  $\beta$ -type tetravacant Dawson-type fragment by eight  $\mu_2\text{-O}$  atoms  $[W\text{-Nd}: 4.045\text{-}4.092 \text{ \AA}]$ , whereas the pentanuclear  $\{Nd_2W_3\}$  cluster is sandwiched by two  $[B\text{-}\alpha\text{-SeW}_9O_{33}]^{8-}$  segments. Additionally, six

crystallographically independent  $Nd^{3+}$  cations ( $Nd1^{3+}$ ,  $Nd2^{3+}$ ,  $Nd3^{3+}$ ,  $Nd4^{3+}$ ,  $Nd5^{3+}$  and  $Nd6^{3+}$ ) in the fourteen-nuclear saddle-shaped  $\{Nd_6W_8\}$  cluster are all octa-coordinate and reside in the distorted square antiprismatic geometry (Fig. 2i). It is worth mentioning that the coordination environments of  $Nd1^{3+}$ ,  $Nd3^{3+}$  and  $Nd4^{3+}$  cations are similar to that of  $Nd^{2+}$ ,  $Nd^{5+}$  and  $Nd^{6+}$  cations, respectively, so only  $Nd1^{3+}$ ,  $Nd3^{3+}$  and  $Nd4^{3+}$  cations are discussed. The  $Nd1^{3+}$  cation is fixed with four terminal water molecules  $[Nd\text{-O}: 2.49(4)\text{-}2.54(4) \text{ \AA}]$ , and four  $\mu_2\text{-O}$  atoms from one tetravacant  $[\beta\text{-Se}_2W_{14}O_{52}]^{12-}$  fragment and two W atoms (W4 and W16)  $[Nd\text{-O}: 2.42(3)\text{-}2.51(3) \text{ \AA}]$ . The  $Nd3^{3+}$  cation, at the apex of the trigonal bipyramid pentanuclear  $\{Nd_2W_3\}$  cluster, is surrounded by three coordination water molecules  $[Nd\text{-O}: 2.43(5)\text{-}2.50(3) \text{ \AA}]$ , two  $\mu_2\text{-O}$  atoms located at one  $[B\text{-}\alpha\text{-SeW}_9O_{33}]^{8-}$  segment  $[Nd\text{-O}: 2.40(3)\text{-}2.50(3) \text{ \AA}]$  and three  $\mu_2\text{-O}$  atoms from three W atoms of the pentanuclear  $\{Nd_2W_3\}$  cluster (W26, W27 and W37)  $[Nd\text{-O}: 2.30(3)\text{-}2.45(3) \text{ \AA}]$ . The  $Nd4^{3+}$  cation coordinates with two water ligands, six  $\mu_2\text{-O}$  atoms from one  $[B\text{-}\alpha\text{-SeW}_9O_{33}]^{8-}$  segment, one  $[\beta\text{-Se}_2W_{14}O_{52}]^{12-}$  fragment and three W atoms  $[Nd\text{-O}: 2.39(3)\text{-}2.60(3) \text{ \AA}]$ . Moreover, in the saddle-shaped

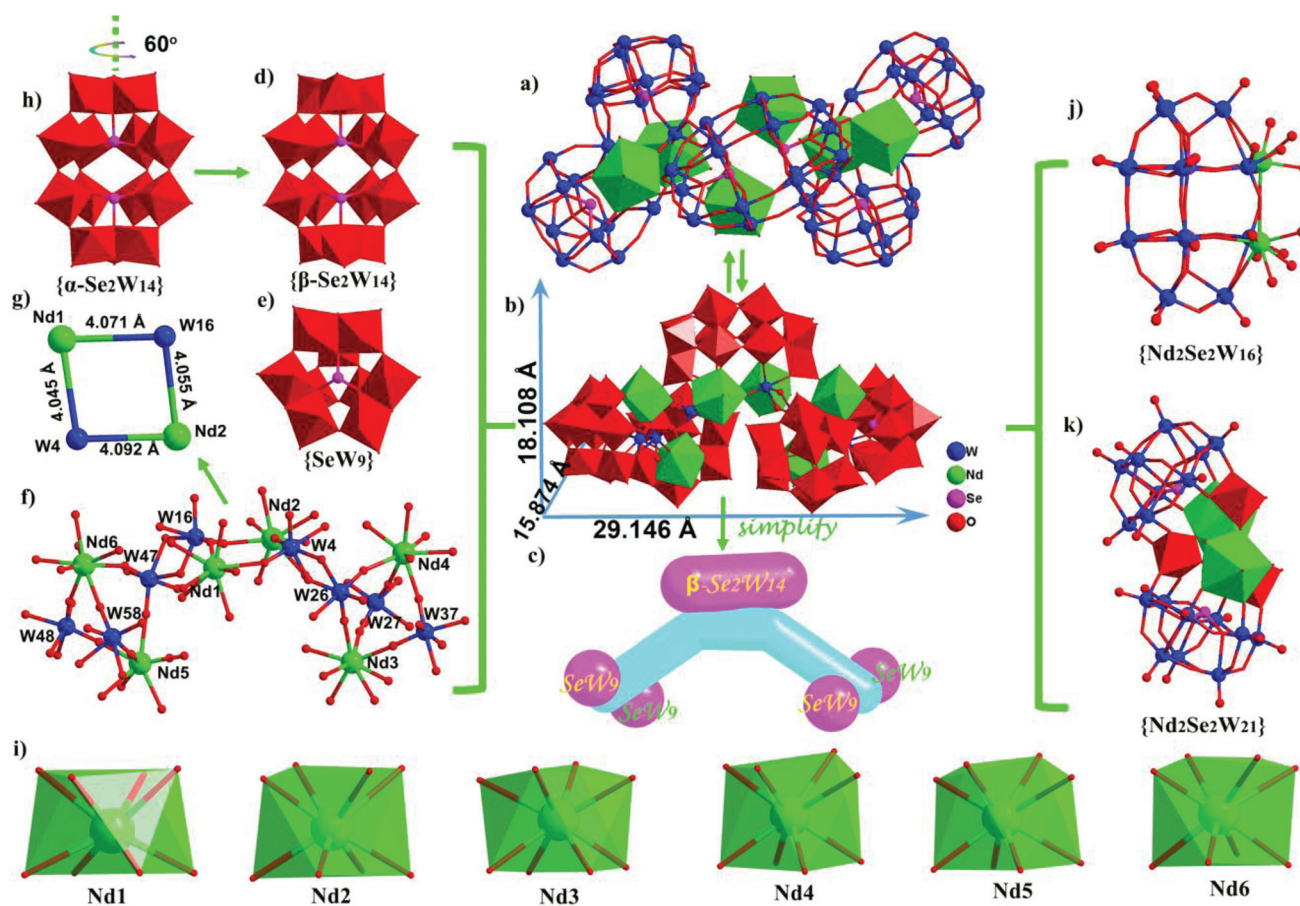


Fig. 2 (a) Ball-and-stick view of the 2a POA. (b) Ball-and-stick/polyhedral view of the 2a POA. (c) Simplified view of the 2a POA. (d) The tetravacant Dawson  $[\beta\text{-Se}_2W_{14}O_{52}]^{12-}$  fragment. (e) The trivacant  $[B\text{-}\alpha\text{-SeW}_9O_{33}]^{8-}$  segment. (f) The saddle-shaped  $\{Nd_6W_8\}$  cluster. (g) The quadrilateral  $\{Nd_2W_2\}$  alignment. (h) The tetravacant Dawson  $[\alpha\text{-Se}_2W_{14}O_{52}]^{12-}$  fragment. (i) The octa-coordinate  $Nd1^{3+}$ - $Nd6^{3+}$  cations of **2**. (j) The  $[Nd_2(H_2O)_8Se_2W_{16}O_{58}(OH)_2]^{8-}$  fragment. (k) The  $[W_3Nd_2(H_2O)_6O_7(SeW_9O_{33})_2]^{6-}$  fragment.

{Nd<sub>6</sub>W<sub>8</sub>} cluster, each hexa-coordinate W atom shows a slightly distorted octahedral geometry [W–O: 1.67(3)–2.32(3) Å].

Poly(POM) species concurrently comprising two different types of HPOT building units are infrequently accounted for, mainly involving cyclic {(Pd<sub>5</sub>Se<sub>2</sub>)(W<sub>3</sub>)(SeW<sub>9</sub>)(Se<sub>2</sub>W<sub>14</sub>)<sub>2</sub>} (4)<sup>17</sup> and sandwich-type {(Zr<sub>3</sub>)(A-α-GeW<sub>9</sub>)(1,4,9-α-P<sub>2</sub>W<sub>15</sub>)}.<sup>41</sup> Among them, 4 was also synthesized by the one-pot reaction strategy under aqueous conditions and contains the same mixed HPOT building units as 2, namely, Keggin-type [B-α-SeW<sub>9</sub>O<sub>33</sub>]<sup>8-</sup> and Dawson-type [β-Se<sub>2</sub>W<sub>14</sub>O<sub>52</sub>]<sup>12-</sup>. And yet there are structurally striking distinctions between them. Apart from the disparity of functional metals incorporated into ST units, the number of Keggin and Dawson fragments is different, 2 consists of four [B-α-SeW<sub>9</sub>O<sub>33</sub>]<sup>8-</sup> segments and one [β-Se<sub>2</sub>W<sub>14</sub>O<sub>52</sub>]<sup>12-</sup> fragment, and 4 is composed of two [B-α-SeW<sub>9</sub>O<sub>33</sub>]<sup>8-</sup> segments and two [β-Se<sub>2</sub>W<sub>14</sub>O<sub>52</sub>]<sup>12-</sup> fragments. Moreover, their molecular configurations are different, 2 has a U-shaped architecture constructed from a central saddle-shaped [W<sub>8</sub>Nd<sub>6</sub>(H<sub>2</sub>O)<sub>20</sub>O<sub>20</sub>(OH)<sub>2</sub>]<sup>24+</sup> cluster encapsulated by five ST units, while in 4, [B-α-SeW<sub>9</sub>O<sub>33</sub>]<sup>8-</sup> and [β-Se<sub>2</sub>W<sub>14</sub>O<sub>52</sub>]<sup>12-</sup> segments are alternately linked by two {Pd<sub>5</sub>Se<sub>2</sub>} clusters and two {W<sub>3</sub>} clusters to form a ring-shaped configuration (Fig. S5†).

Additionally, it is not hard to see that most of reported poly (POM) aggregates contain an even number of HPOT building units per molecular unit, such as dimer, tetramer, hexamer, octamer, *etc.* In contrast, except for monomeric and trimeric POM aggregates, surprisingly, little literature has been documented on poly(POM) species composed of more odd number of HPOT building units. Thereby, the discovery of nanosized pentameric ST 2 enriches the structural variety in this aspect.

Alternatively, the 2a POA can be also perceived as the integration of a di-nuclear Nd<sup>3+</sup>-containing divacant [Nd<sub>2</sub>(H<sub>2</sub>O)<sub>8</sub>Se<sub>2</sub>W<sub>16</sub>O<sub>58</sub>(OH)<sub>2</sub>]<sup>8-</sup> (Fig. 2j) fragment with two pentanuclear heterometallic cluster sandwiched dimers [W<sub>3</sub>Nd<sub>2</sub>(H<sub>2</sub>O)<sub>6</sub>O<sub>7</sub>(SeW<sub>9</sub>O<sub>33</sub>)<sub>2</sub>]<sup>6-</sup> (Fig. 2k) through W–O–W and W–O–Nd linkers. In addition, the 2a POA can also be described as a pentamer that comprises a hexavacant [β-Se<sub>2</sub>W<sub>12</sub>O<sub>46</sub>]<sup>12-</sup> fragment and four trivacant [B-α-SeW<sub>9</sub>O<sub>33</sub>]<sup>8-</sup> segments anchoring a sixteen-nuclear [Nd<sub>6</sub>W<sub>10</sub>(H<sub>2</sub>O)<sub>20</sub>O<sub>26</sub>(OH)<sub>2</sub>]<sup>24+</sup> {Nd<sub>6</sub>W<sub>10</sub>} heterometallic cluster by virtue of 32 μ<sub>2</sub>-O and 2 μ<sub>4</sub>-O atoms (Fig. 3a–c). Although it has not yet been isolated, the hexavacant [β-Se<sub>2</sub>W<sub>12</sub>O<sub>46</sub>]<sup>12-</sup> fragment exists in reported vacant Dawson derivatives.<sup>42,43</sup> The {Nd<sub>6</sub>W<sub>10</sub>} cluster can be perceived as a [Nd<sub>2</sub>W<sub>4</sub>(H<sub>2</sub>O)<sub>8</sub>O<sub>12</sub>(OH)<sub>2</sub>]<sup>4+</sup> {Nd<sub>2</sub>W<sub>4</sub>} subcluster connecting two identical pentanuclear [Nd<sub>2</sub>W<sub>3</sub>(H<sub>2</sub>O)<sub>6</sub>O<sub>7</sub>]<sup>10+</sup> {Nd<sub>2</sub>W<sub>3</sub>} subclusters (Fig. 3d–f), and the distances of W47–W16 and Nd6–W15 are 3.274 Å and 3.946 Å, respectively (Fig. 3g). In the {Nd<sub>2</sub>W<sub>4</sub>} alignment (Fig. 3h), the distances of W–W linked by μ<sub>2</sub>-O atoms are 3.777 Å (W16–W15) and 3.794 Å (W4–W35), respectively, and the Nd–W distances vary from 4.040 to 4.109 Å. Both pentanuclear {Nd<sub>2</sub>W<sub>3</sub>} clusters (Fig. 3d and e) present the trigonal bipyramidal geometry and the distances of Nd–W fall in 4.045–4.180 Å.

It can be observed from the 3D stacking diagram that 2a POAs are arranged in the fashion of –A–A– with a distance of 19.62 Å viewed along the *a* axis, and show the –A–B–A–

arrangement mode along the *b* and *c* axes with the distances of 28.53 Å and 30.01 Å, respectively (Fig. 3i and j, S6†).

### Catalytic oxidation properties

Catalytic oxidation is one of the most important chemical processes in a broad range of catalytic fields.<sup>44,45</sup> The oxygenated products bearing versatile functional groups (such as epoxides, alcohols, aldehydes, ketones, and carboxylic acids) have frequently been used as intermediates. During the oxidation process, the choice of oxidant is of great importance; H<sub>2</sub>O<sub>2</sub>, as an environmentally friendly oxidant, has the following advantages compared to traditional oxidants; (1) high contents of active oxygen species; (2) producing H<sub>2</sub>O as the sole by-product; (3) relatively low cost; and (4) more stable and ready availability.<sup>46–48</sup> Therefore, H<sub>2</sub>O<sub>2</sub> as a “green” oxygen donor is highly favored. However, the oxidation process of H<sub>2</sub>O<sub>2</sub> as an oxidant usually requires a catalyst. POMs have been widely applied to the catalytic field due to the instinct traits of high activity and stability, controllable redox and acidity properties, inherent resistance to oxidative decomposition and impressive sensitivity to light and electricity.<sup>49,50</sup> These prominent advantages are closely related to their structures and compositions. Therefore, it is significant to design and prepare POM catalysts that possess novel structures and outstanding catalytic performances under mild conditions.

Selective oxidation of thioethers, as a type of organic oxidation, is a meaningful and pivotal reaction due to the oxygenated products (sulfones and sulfoxides) owning versatile utilities in the chemical industry, medicinal chemistry and biochemistry, *etc.* Thioethers can be effectively oxidized with H<sub>2</sub>O<sub>2</sub> to produce the corresponding oxidation products in the presence of POMs as catalysts.<sup>51–53</sup> Here, 2 as a heterogeneous catalyst was investigated in the oxidation of various aromatic thioethers with H<sub>2</sub>O<sub>2</sub> in an acetonitrile (CH<sub>3</sub>CN) solvent (Scheme 1). The products of thioether oxidation were recognized by GC-MS spectra and the selectivity of sulfoxide and sulfone as well as the conversion of thioethers were identified by GC spectra.

For the initial experiment, methyl phenyl sulfide (MPS) was selected as a substrate to evaluate the catalytic performance of 2 as a catalyst at 35 °C under the conditions of 3 mL of CH<sub>3</sub>CN as the solvent, 0.5 mmol substrate, a 3 oxidant/substrate (O/S) molar ratio, a 500 substrate/catalyst (S/C) molar ratio and a reaction time of 1 h. Experimental results indicate that MPS has been completely oxidized to MPSO<sub>2</sub>, showing 100% conversion and 100% selectivity (Fig. 4a). Considering the influence of reaction time on the catalytic oxidation of thioethers, we attempted to vary reaction time under identical conditions. Monitoring the experiments every 10 min, surprisingly, we found that the reaction time could be shortened to 10 min for a complete conversion of MPS with 100% selectivity for MPSO<sub>2</sub> (Fig. 4a), which is much faster than those similar reactions reported using POMs as catalysts (the reported reaction time for the catalytic oxidation of MPS is usually 60 min) (Table S3†). Similarly, diphenyl sulfide (DPS) as a substrate

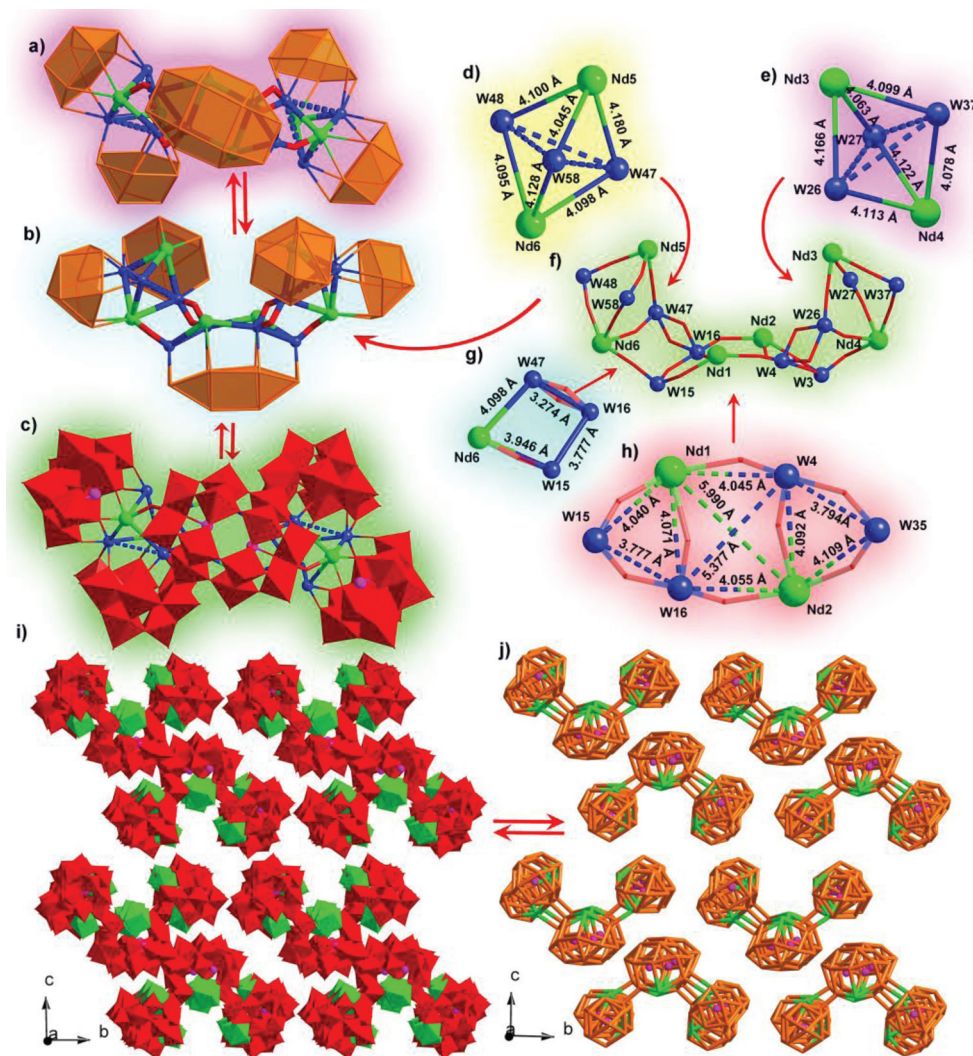
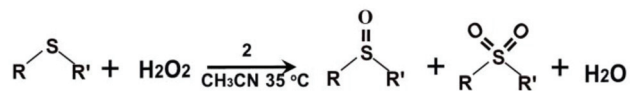


**Fig. 3** (a and b) Simplified views of the **2a** POA in different orientations. (c) View of the **2a** POA. (d and e) Two simplified pentanuclear  $\{Nd_2W_3\}$  sub-clusters in the trigonal bipyramidal arrangement. (f) The simplified  $\{Nd_6W_{10}\}$  cluster. (g) View of the distribution of W47, W16, W15 and Nd6. (h) View of the distribution of W15, Nd1, W4, W35, Nd2 and W16. (i) View of the stacking of **2a** POAs along the *a* axis. (j) Simplified view of the stacking of **2a** POAs along the *a* axis.



**Scheme 1** Catalytic oxidation of thioethers.

was also investigated, which also shows 100% conversion and 100% selectivity for DPSO<sub>2</sub> in 10 min (Fig. 4b).

Motivated by the above prominent experimental results of **2** as a catalyst, under the optimized conditions (3 O/S, 500 S/C, 3 mL of CH<sub>3</sub>CN, 35 °C, 10 min), catalytic measurements of **2** were extended to various aromatic thioethers. It is well known that the introduction of substituent groups with different electron effects and steric hindrance usually has some striking influences on catalyses in organic reactions. Herein,

different thioether substrates were chosen based on the following considerations: (1) investigate the effect of introduced electron-donating/electron-withdrawing groups on aromatic thioethers on the conversion and selectivity (entries 5–7); (2) explore the effect of the position of the substituents of aryl thioethers on the formation of sulfones and sulfoxides (entries 7–9); and (3) detect the influence of the steric hindrance effect on the conversion of oxidation products (entries 1, 3, 11 and 12). As can be observed in Table 2, catalytic oxidations of other ten aromatic thioethers were successfully achieved by making use of **2** as a catalyst under the same conditions. It is worth mentioning that all selected thioethers including diphenyl sulfide, dibenzothiophene, 2-bromo-thioanisole, benzothiophene and 2-methylbenzo-thiophene can be almost oxidized to the corresponding sulfones in 10 min and exhibit excellent selectivity. These results indicate that electron-donating/elec-

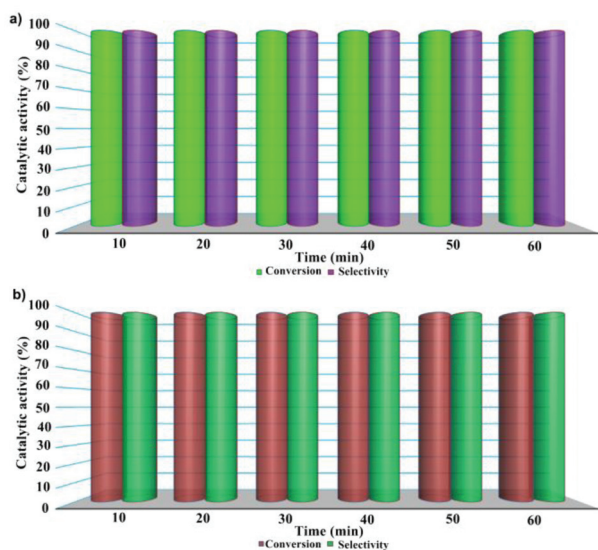


**Fig. 4** (a) and (b) The conversion of MPS and DPS and the selectivity of  $\text{MPSO}_2$  and  $\text{DPSO}_2$  at different reaction times under reaction conditions: 0.5 mmol substrate, 3 O/S molar ratio, 500 S/C molar ratio, 3 mL acetonitrile, at 35 °C.

tron-withdrawing groups on aromatic thioethers and steric hindrance of the substituent groups have negligible influence on the conversion and the selectivity compared with those previously reported results,<sup>10,29,51–58</sup> suggesting that the outstand-

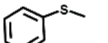
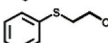
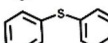
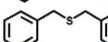
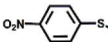
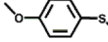
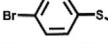
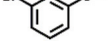
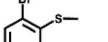
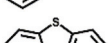
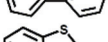
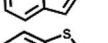
ing oxidation performance of aromatic thioethers is rare in the catalytic system of POMs (Table 3). It is easy to be observed that when compared with  $[\text{Zr}_{24}\text{O}_{22}(\text{OH})_{10}(\text{H}_2\text{O})_2(\text{W}_2\text{O}_{10}\text{H})_2(\text{GeW}_9\text{O}_{34})_4(\text{GeW}_8\text{O}_{31})_2]^{32-}$ ,<sup>10</sup>  $[\text{Ce}_2(\text{H}_2\text{O})_6(\text{DMEA})\text{W}_4\text{O}_9(\alpha\text{-SeW}_9\text{O}_{33})_3]^{12-}$ ,<sup>29</sup>  $[\text{Ce}_2\text{W}_4\text{O}_9(\text{H}_2\text{O})_7(\text{SeW}_9\text{O}_{33})_3]^{24-}$ ,<sup>29</sup>  $[\text{As}_4\text{W}_{40}\text{O}_{140}\{\text{Ru}_2(\text{CH}_3\text{COO})\}_2]^{14-}$ ,<sup>54</sup> *etc.*, **2** exhibits better catalytic performance, which may be related to the presence of more protonated oxygen atoms in the architecture of **2**. Protons are required to generate the active peroxy species, and here, the presence of numerous protonated oxygen atoms on the W and Nd atoms facilitates the generation of the most probable hydroperoxy POM complex, which rapidly and efficiently promotes the oxidation of thioethers.<sup>59</sup>

The recyclability of catalyst **2** was also investigated by the cyclic oxidation reactions of MPS. At the end of each reaction, the catalyst was filtered for recycling. After five cycles, **2** still exhibits satisfactory catalytic activity in the experiments (the conversion of MPS is higher than 91% and the selectivity of  $\text{MPSO}_2$  is 100% in the fifth cycle) (Fig. 5).

Furthermore, the stability of **2** during the catalytic reaction was verified by the good agreements of the characteristic  $\nu(\text{W}-\text{O}_t)$ ,  $\nu(\text{Se}-\text{O})$ ,  $\nu(\text{W}-\text{O}_b)$  and  $\nu(\text{W}-\text{O}_c)$  vibration patterns derived from the ST skeletons in the IR spectra of the fresh **2** and recycled catalysts (Fig. S9†).

Although the catalytic mechanism of **2** as a catalyst is not well understood, according to our experimental results and the previous reports, we speculate that the oxidant  $\text{H}_2\text{O}_2$  first interacts with the terminal metal–oxo bonds in the POA of **2**

**Table 2** Selective oxidation of various aromatic thioethers to sulfones

Entry	Substrate	Time (min)	Temperature (°C)	Conversion (%)	Selectivity (%) RR'SO/R'RSO <sub>2</sub>	
1		10	35	100	0	100
2		10	35	100	1	99
3		10	35	100	0	100
4		10	35	100	0	100
5		10	35	100	0	100
6		10	35	100	0	100
7		10	35	100	0	100
8		10	35	100	0	100
9		10	35	100	0	100
10		10	35	100	1	99
11		10	35	99	0	100
12		10	35	100	1	99

Catalytic experimental conditions: substrate (0.5 mmol), 3 O/S, 500 S/C,  $\text{CH}_3\text{CN}$  (3 mL), 35 °C, 10 min.



Table 3 Comparison of the catalytic oxidation performance of some POM-based catalysts with compound 2

Compounds	Conv/Sel	Temp (°C) /time (min)	Conv/Sel	Temp (°C) /time (min)	Conv/Sel	Temp (°C) /time (min)	Ref.
$[Zr_{2.4}O_{2.2}(\text{OH})_{10}(\text{H}_2\text{O})_2(\text{W}_2\text{O}_{10}\text{H})_2(\text{CeW}_9\text{O}_{34})_4(\text{GeW}_8\text{O}_{31})_2]^{32-}$	45/27	60/60	69/10	60/60	Trace	60/60	10
$[\text{Ce}_2(\text{H}_2\text{O})_6(\text{DMEA})\text{W}_4\text{O}_9(\alpha\text{-SeW}_9\text{O}_{33})_3]^{12-}$	100/100	40/60	100/100	40/60	99/100	40/60	29
$[\text{Ce}_2\text{W}_4\text{O}_8(\text{H}_2\text{O})_7(\text{SeW}_9\text{O}_{33})_2]^{24-}$	100/100	40/60	100/100	40/60	98/100	40/60	29
$[\text{Ln}_3(\text{H}_2\text{O})_{14}(\text{Mo}_8\text{O}_{24})(\text{O}_3\text{PCH}_2\text{COO})_3]^{9-}$	100/99	50/120	—	—	68.5/100	60/180	51
$[\text{As}_4\text{W}_{40}\text{O}_{140}(\text{Ru}_2(\text{CH}_3\text{COO}))_2]^{14-}$	99/97	50/90	—	—	52/98.5	50/180	54
$\{\text{Ti}_7\text{O}_6(\text{SbW}_9\text{O}_{33})_4\}^{40-}$	100/59	50/60	100/8	50/60	11/45	50/60	56
$\{\text{Ti}_7\text{O}_6(\text{SbW}_9\text{O}_{33})_4\}^{40-}$	100/100	60/60	100/71	60/180	92/99	60/180	56
$[\{\text{Re}(\text{CO})_3(\text{Mo}_4\text{O}_{16})\}]^{14-}$	94/20	35/90	—	—	—	—	57
$[\text{Na}_2\text{Sb}_4(\text{Sb}_2\text{Mo}_{12}\text{O}_{57})]^{12-}$	98/95	25/600	—	—	—	—	58
$\{\text{W}_2\text{Nd}_2(\text{H}_2\text{O})_8\text{O}_6(\text{OH})_2(\beta\text{-Se}_3\text{W}_{14}\text{O}_{52})\}[\text{W}_3\text{Nd}_2(\text{H}_5\text{O})_6\text{O}_7(\beta\text{-}\alpha\text{-SeW}_9\text{O}_{33})_2]^{20-}$	100/100	35/10	100/100	35/10	99/100	35/10	This paper

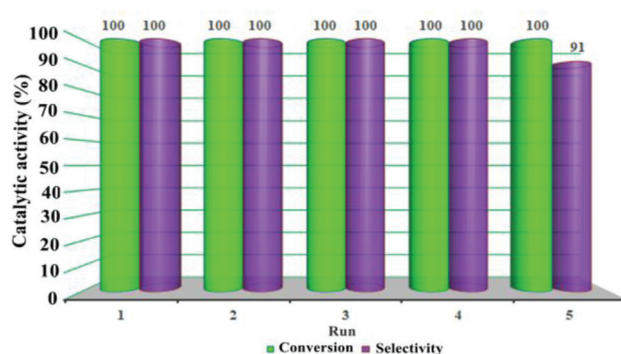


Fig. 5 Recycling of the catalytic oxidation of MPS in the presence of 2.

(especially the protonated W–OH, W–OH<sub>2</sub> or Nd–H<sub>2</sub>O) to rapidly form the active peroxide POM species and then transfers the active O atoms to aromatic thioethers or sulfoxides, and the terminal metal–oxo bonds are recovered and can be used to restart the catalytic cycle (Fig. S10†). This catalytic mechanism is similar to the previous results.<sup>60–62</sup>

## Conclusions

In summary, two novel Nd<sup>3+</sup> substituted poly(ST) aggregates containing mixed Keggin and Dawson fragments have been synthesized by utilizing the structure-directing effect of a trigonal pyramidal {SeO<sub>3</sub>} template using the one-pot self-assembly strategy in a conventional aqueous solution. The successful preparations of 1 and 2 hold promise for further exploring nanosized poly(POM) aggregates including two or more kinds of architecturally distinct HPOT units. Furthermore, the existence of some protonated oxygen atoms in the POA structure of 2 enables it to achieve highly efficient catalytic oxidation of aromatic thioethers in a very short time, which manifests the vast potential of STs in catalytic oxidation reaction. This work not only enriches the structural diversity of POM family, but also provides an opportunity for expanding the potential applications of POM-based materials. Further explorations on the combination of different metals and the other lone-electron pair stereochemical effect groups (*e.g.*, {AsO<sub>3</sub>}, {SbO<sub>3</sub>}, {BiO<sub>3</sub>} and {TeO<sub>3</sub>}, which can structurally direct the aggregation of {WO<sub>6</sub>} units into multiple lacunary POM nucleophiles instead of the undesired saturated configurations, allowing the construction of novel POMs) are underway in our laboratory.

## Conflicts of interest

There are no conflicts of interest to declare.

## Acknowledgements

This work was supported by the National Natural Science Foundation of China (21871077, 21671054, 21571048 and

21771052), the Program for Innovation Teams in Science and Technology in the Universities of Henan Province (20IRTSTHN004) and the Program of First-Class Discipline Cultivation Project of Henan University (2019YLZDYJ02).

## Notes and references

- 1 A. Rezaeifard, R. Haddad, M. Jafarpour and M. Hakimi, *ACS Sustainable Chem. Eng.*, 2014, **2**, 942–950.
- 2 M. C. Carreno, *Chem. Rev.*, 1995, **95**(17), 17–1760.
- 3 S. Caron, R. W. Dugger, S. G. Ruggeri, J. A. Ragan and D. H. B. Ripin, *Chem. Rev.*, 2006, **106**, 2943–2989.
- 4 H. L. Holland, *Chem. Rev.*, 1988, **88**, 473–485.
- 5 T. Uematsu, Y. Miyamoto, Y. Ogasawara, K. Suzuki, K. Yamaguchi and N. Mizuno, *Catal. Sci. Technol.*, 2016, **6**, 222–233.
- 6 C. Wang, Z. G. Chen, X. Y. Yao, Y. H. Chao, S. H. Xun, J. Xiong, L. Fan, W. S. Zhu and H. M. Li, *Fuel*, 2018, **230**, 104–112.
- 7 A. M. Khenkin and R. Neumann, *J. Am. Chem. Soc.*, 2002, **124**, 4198–4199.
- 8 Y. Wang, K. Kamata, R. Ishimoto, Y. Ogasawara, K. Suzuki, K. Yamaguchi and N. Mizuno, *Catal. Sci. Technol.*, 2015, **5**, 2602–2611.
- 9 R. Fareghi-Alamdari, S. M. Hafshejani, H. Taghiyar, B. Yadollahi and M. R. Farsani, *Catal. Commun.*, 2016, **78**, 64–67.
- 10 L. Huang, S.-S. Wang, J.-W. Zhao, L. Cheng and G.-Y. Yang, *J. Am. Chem. Soc.*, 2014, **136**, 7637–7642.
- 11 H.-L. Li, Y.-J. Liu, J.-L. Liu, L.-J. Chen, J.-W. Zhao and G.-Y. Yang, *Chem. – Eur. J.*, 2017, **23**, 2673–2689.
- 12 J. Dong, J. F. Hu, Y. N. Chi, Z. G. Lin, B. Zou, S. Yang, C. L. Hill and C. W. Hu, *Angew. Chem., Int. Ed.*, 2017, **56**, 4473–4477.
- 13 D. Wang, L. L. Liu, J. Jiang, L. J. Chen and J. W. Zhao, *Nanoscale*, 2020, **12**, 5705–5718.
- 14 J.-C. Liu, Q. Han, L.-J. Chen, J.-W. Zhao, C. Streb and Y.-F. Song, *Angew. Chem., Int. Ed.*, 2018, **57**, 8416–8420.
- 15 J. M. Cameron, J. Gao, L. Vilà-Nadal, D.-L. Long and L. Cronin, *Chem. Commun.*, 2014, **50**, 2155–2157.
- 16 Y. Zhang, J. Jiang, Y. F. Liu, P. Li, Y. Liu, L. J. Chen and J. W. Zhao, *Nanoscale*, 2020, **12**, 10842–10853.
- 17 J. M. Cameron, J. Gao, D.-L. Long and L. Cronin, *Inorg. Chem. Front.*, 2014, **1**, 178–185.
- 18 J. Yan, D.-L. Long and L. Cronin, *Angew. Chem., Int. Ed.*, 2010, **49**, 4117–4120.
- 19 I. V. Kalinina, E. V. Peresyphkina, N. V. Izarova, F. M. Nkala, U. Kortz, N. B. Kompankov, N. K. Moroz and M. N. Sokolov, *Inorg. Chem.*, 2014, **53**, 2076–2082.
- 20 J. Gao, J. Yan, S. Beeg, D.-L. Long and L. Cronin, *J. Am. Chem. Soc.*, 2013, **135**, 1796–1805.
- 21 J. Yan, J. Gao, D.-L. Long, H. N. Miras and L. Cronin, *J. Am. Chem. Soc.*, 2010, **132**, 11410–11411.
- 22 Y. Zhang, Y. M. Li, J. J. Pang, Y. F. Liu, P. Li, L. J. Chen and J. W. Zhao, *Inorg. Chem.*, 2019, **58**, 7078–7090.
- 23 W.-C. Chen, C. Qin, X.-L. Wang, Y.-G. Li, H.-Y. Zang, Y.-Q. Jiao, P. Huang, K.-Z. Shao, Z.-M. Su and E.-B. Wang, *Chem. Commun.*, 2014, **50**, 13265–13267.
- 24 W.-C. Chen, C. Qin, X.-L. Wang, K.-Z. Shao, Z.-M. Su and E.-B. Wang, *Cryst. Growth Des.*, 2016, **16**, 2481–2486.
- 25 W.-C. Chen, H.-L. Li, X.-L. Wang, K.-Z. Shao, Z.-M. Su and E.-B. Wang, *Chem. – Eur. J.*, 2013, **19**, 11007–11015.
- 26 H. L. Li, W. Yang, Y. Chai, L. J. Chen and J. W. Zhao, *Inorg. Chem. Commun.*, 2015, **56**, 35–40.
- 27 H. L. Li, Y. J. Liu, Y. M. Li, L. J. Chen, J. W. Zhao and G. Y. Yang, *Chem. – Asian J.*, 2018, **13**, 2897–2907.
- 28 Y. J. Liu, H. L. Li, C. T. Lu, P. J. Gong, X. Y. Ma, L. J. Chen and J. W. Zhao, *Cryst. Growth Des.*, 2017, **17**, 3917–3928.
- 29 H.-L. Li, C. Lian, L.-J. Chen, J.-W. Zhao and G.-Y. Yang, *Inorg. Chem.*, 2019, **58**, 8442–8450.
- 30 W.-C. Chen, L.-K. Yan, C.-X. Wu, X.-L. Wang, K.-Z. Shao, Z.-M. Su and E.-B. Wang, *Cryst. Growth Des.*, 2014, **14**, 5099–5110.
- 31 W.-C. Chen, C.-Q. Jiao, X.-L. Wang, K.-Z. Shao and Z.-M. Su, *Inorg. Chem.*, 2019, **58**, 12895–12904.
- 32 I. D. Brown and D. Altermatt, *Acta Crystallogr., Sect. B: Struct. Sci.*, 1985, **41**, 244–247.
- 33 H. L. Li, Y. J. Liu, R. Zheng, L. J. Chen, J. W. Zhao and G. Y. Yang, *Inorg. Chem.*, 2016, **55**, 3881–3893.
- 34 Z. M. Zhang, S. Yao, Y. G. Li, H. H. Wu, Y. H. Wang, M. Rouzières, R. Clérac, Z. M. Su and E. B. Wang, *Chem. Commun.*, 2013, **49**, 2515–2517.
- 35 Z. M. Zhang, Y. G. Li, E. B. Wang, X. L. Wang, C. Qin and H. Y. An, *Inorg. Chem.*, 2006, **45**, 4313–4315.
- 36 C. Pichon, P. Mialane, A. Dolbecq, J. Marrot, E. Rivière, B. S. Bassil, U. Kortz, B. Keita, L. Nadjjo and F. Sécheresse, *Inorg. Chem.*, 2008, **47**, 11120–11128.
- 37 Y. Huo, R. Wan, P. T. Ma, J. L. Liu, Y. C. Chen, D. D. Li, J. Y. Niu, J. P. Wang and M.-L. Tong, *Inorg. Chem.*, 2017, **56**, 12687–12691.
- 38 J.-W. Zhao, H.-L. Li, X. Ma, Z. G. Xie, L.-J. Chen and Y. S. Zhu, *Sci. Rep.*, 2016, **6**, 26406.
- 39 M. Ibrahim, S. S. Mal, B. S. Bassil, A. Banerjee and U. Kortz, *Inorg. Chem.*, 2011, **50**, 956–960.
- 40 X. Xu, R. R. Meng, C. T. Lu, L. Mei, L. J. Chen and J. W. Zhao, *Inorg. Chem.*, 2020, **59**(6), 3954–3963.
- 41 Z. Zhang, J.-W. Zhao and G.-Y. Yang, *Eur. J. Inorg. Chem.*, 2017, 3244–3247.
- 42 J. M. Cameron, J. Gao, L. Vilà-Nadal, D.-L. Long and L. Cronin, *Chem. Commun.*, 2014, **50**, 2155–2157.
- 43 I. V. Kalinina, E. V. Peresyphkina, N. V. Izarova, F. M. Nkala, U. Kortz, N. B. Kompankov, N. K. Moroz and M. N. Sokolov, *Inorg. Chem.*, 2014, **53**, 2076–2082.
- 44 E. Takahashi, K. Kamata, Y. Kikukawa, S. Sato, K. Suzuki, K. Yamaguchia and N. Mizuno, *Catal. Sci. Technol.*, 2015, **5**, 4778–4789.
- 45 J. H. Tong, W. H. Wang, L. D. Su, Q. Li, F. F. Liu, W. M. Ma, Z. Q. Lei and L. L. Bo, *Catal. Sci. Technol.*, 2017, **7**, 222–230.
- 46 Z.-J. Lin, H.-Q. Zheng, J. Chen, W.-E. Zhuang, Y.-X. Lin, J.-W. Su, Y.-B. Huang and R. Cao, *Inorg. Chem.*, 2018, **57**, 13009–13019.

- 47 S. Doherty, J. G. Knight, M. A. Carroll, J. R. Ellison, S. J. Hobson, S. Stevens, C. Hardacre and P. Goodrich, *Green Chem.*, 2015, **17**, 1559–1571.
- 48 C. Shen, Y. J. Wang, J. H. Xu and G. S. Luo, *Green Chem.*, 2016, **18**, 771–781.
- 49 A. Nisar, J. Zhuang and X. Wang, *Adv. Mater.*, 2011, **23**, 1130–1135.
- 50 C. F. Li, K. Suzuki, N. Mizuno and K. Yamaguchi, *Chem. Commun.*, 2018, **54**, 7127–7130.
- 51 J. W. Wang, Y. J. Niu, M. Zhang, P. T. Ma, C. Zhang, J. Y. Niu and J. P. Wang, *Inorg. Chem.*, 2018, **57**, 1796–1805.
- 52 M. Carraro, N. Nsouli, H. Oelrich, A. Sartorel, A. Sorarù, S. S. Mal, G. Scorrano, L. Walder, U. Kortz and M. Bonchio, *Chem. – Eur. J.*, 2011, **17**, 8371–8378.
- 53 O. A. Kholdeeva, G. M. Maksimov, R. I. Maksimovskaya, L. A. Kovaleva, M. A. Fedotov, V. A. Grigoriev and C. L. Hill, *Inorg. Chem.*, 2000, **39**, 3828–3837.
- 54 M. D. Han, Y. J. Niu, R. Wan, Q. F. Xu, J. K. Lu, P. T. Ma, C. Zhang, J. Y. Niu and J. P. Wang, *Chem. – Eur. J.*, 2018, **24**, 11059–11066.
- 55 Y. J. Niu, Q. F. Xu, Y. Wang, Z. Li, J. K. Lu, P. T. Ma, C. Zhang, J. Y. Niu and J. P. Wang, *Dalton Trans.*, 2018, **47**, 9677–9684.
- 56 H.-L. Li, C. Lian, D.-P. Yin, Z.-Y. Jia and G.-Y. Yang, *Cryst. Growth Des.*, 2019, **19**, 376–380.
- 57 J. K. Lu, X. Y. Ma, V. Singh, Y. J. Zhang, P. T. Ma, C. Zhang, J. Y. Niu and J. P. Wang, *Dalton Trans.*, 2018, **47**, 5279–5285.
- 58 J. K. Lu, Y. P. Wang, X. Y. Ma, Y. J. Niu, V. Singh, P. T. Ma, C. Zhang, J. Y. Niu and J. P. Wang, *Dalton Trans.*, 2018, **47**, 8070–8077.
- 59 O. A. Kholdeeva, G. M. Maksimov, R. I. Maksimovskaya, L. A. Kovaleva, M. A. Fedotov, V. A. Grigoriev and C. L. Hill, *Inorg. Chem.*, 2000, **39**, 3828–3837.
- 60 S. Ribeiro, C. M. Granadeiro, P. Silva, F. A. A. Paz, F. F. de Biani, L. Cunha-Silva and S. S. Balula, *Catal. Sci. Technol.*, 2013, **3**, 2404–2414.
- 61 A. Nisar, Y. Lu, J. Zhuang and X. Wang, *Angew. Chem., Int. Ed.*, 2011, **50**, 3187–3192.
- 62 Y. Guo, J. W. Fu, L. Li, X. N. Li, H. Y. Wang, W. W. Ma and H. Zhang, *Inorg. Chem. Front.*, 2018, **5**, 2205–2210.